

## Efficient Conditional Preparation of High-Fidelity Single Photon States for Fiber-Optic Quantum Networks

Alfred B. U'Ren,<sup>1,2</sup> Christine Silberhorn,<sup>1</sup> Konrad Banaszek,<sup>1</sup> and Ian A. Walmsley<sup>1</sup>

<sup>1</sup>*Clarendon Laboratory, Oxford University, Parks Road, Oxford, OX1 3PU, United Kingdom*

<sup>2</sup>*The Institute of Optics, University of Rochester, Rochester, New York 14627, USA*

(Received 12 December 2003; published 25 August 2004)

Highly correlated photons or, accordingly, high-fidelity single-photon states are a prerequisite for closing detection loopholes in experimental tests of local realism and implementing scalable linear optical quantum computation. We demonstrate a parametric down-conversion source exhibiting a conditional *detection* efficiency of 51% (with corresponding *preparation* efficiency of 85%) and extraordinarily high detection rates of up to  $8.5 \times 10^5$  coincidences/(smW). We exploit a novel type-II phase matching configuration in a microstructured waveguide in conjunction with an ultrashort pump.

DOI: 10.1103/PhysRevLett.93.093601

PACS numbers: 42.50.Dv, 03.67.Lx

Single photons provide an important bridge between classical and nonclassical physics. For example, it is possible to define a single-photon wave function that has exactly the same form as the classical electromagnetic field [1], yet exhibits a singular or nonpositive quadrature phase-space representation [2]. Single photons are also important in quantum information processing, where they can serve as qubits in quantum cryptographic links and in quantum computers. In such applications, a very high degree of correlation between the photons serving as the quantum register is vital. The successful operation of a gate in a linear optical quantum computer (LOQC) [3], for example, is heralded by the firing of an ancillary detector. Imperfect heralding reduces the fidelity of the gate operation, since it leads to a contaminatory vacuum contribution to the prepared output state. This can be removed only by postselection of the state by coincidence measurements, which precludes scaling. Likewise, the efficient collection of correlated photon pairs is required for tests of local realism, such as the strong violation of Bell's inequality [4]. If photon-pair members randomly escape detection, a detection "loop-hole" exists that necessitates auxiliary assumptions about the quantum state of the postselected subensemble. Recent progress in the demonstration of an all-optical two-qubit quantum logic gate for LOQC highlights the benefits of high-fidelity single-photon sources [5]. At the heart of the gate operation is quantum interference, which requires photonic wave packets exhibiting well-defined modal character. Indeed, modal distinguishability hinders the implementation not only of LOQC but of all schemes relying on interference of photons from multiple sources [6], such as teleportation [7], entanglement swapping [8], and networking via quantum repeaters [9]. Furthermore, single-photon emission in well-defined modes permits efficient fiber coupling, which is crucial for long-haul quantum cryptography [10].

Two distinct approaches for generating single photons are currently being pursued: deterministic sources of single photons emitted on demand and spontaneous sources based on photon-pair generation where a single-photon is prepared by detection of the conjugate pair member. Sources based on single vacancy centers [11], quantum dots [12], atoms in cavities [13] and molecular emission [14] emit photons deterministically and often rely on intricate experimental setups (e.g., cryogenic cooling). For solid-state sources, however, it remains a challenge to control the emission modes, resulting in poor interference, poor fiber coupling, and low detection efficiencies, thus leading to a random selection of collected photons. In the process of parametric down-conversion (PDC), on the other hand, photon-pair emission occurs randomly but the presence of a single photon can be determined by the detection of its sibling. It is nevertheless difficult to collect the entire photon sample from bulk crystals [15] due to the relatively complicated spatial emission pattern. PDC from quasi-phase-matched (QPM) nonlinear waveguides has recently been shown, however, to exhibit emission in controlled modes defined by the guide [16]. Accurate spatial mode definition leads to efficient optical fiber coupling and to high-visibility interference. A fundamental requirement for high-fidelity conditional preparation of single photons based on waveguided PDC is efficient pair splitting, which is realized here through a nonlinear interaction producing orthogonally polarized (and therefore spatially separable) photon pairs.

The difficulty in generating orthogonally polarized PDC light in a waveguided  $\chi^{(2)}$  interaction is that existing waveguide structures are commonly designed to take advantage of the high  $d_{33}$  nonlinearities of LiNbO<sub>3</sub> and KTiOPO<sub>4</sub> (KTP), which implies the use of type-I phase matching yielding same-polarization photon pairs. Since waveguiding additionally implies that both photons in a

given pair occupy a waveguide-supported spatial mode, it is challenging to split the pairs. For common  $\chi^{(2)}$  materials such as quasi-phase-matched LiNbO<sub>3</sub>, waveguiding supports only one polarization. Thus, to date, quantum-optical experiments making use of nonlinear waveguides have employed type-I phase matching [16,17]. We have designed a type-II PDC interaction in a quasi-phase-matched KTP waveguide leading to much improved conditional detection rates and to easily separable (by means of their polarization) photon pairs. In such a phase matching configuration (utilizing the  $\chi^{(2)}$  element  $d_{24}$ ), a horizontally polarized ultraviolet photon spontaneously decays into two infrared photons, horizontally and vertically polarized.

Our experimental apparatus is depicted in Fig. 1. The output of a mode-locked titanium sapphire laser (100 fs pulse duration, 87 MHz repetition rate) is directed to a 2 mm long  $\beta$ -barium-borate crystal yielding pulses centered at 400.5 nm, whose bandwidth is restricted by an interference filter with a FWHM of 2 nm. This ultraviolet beam (power measured before coupling was 15  $\mu$ W) is

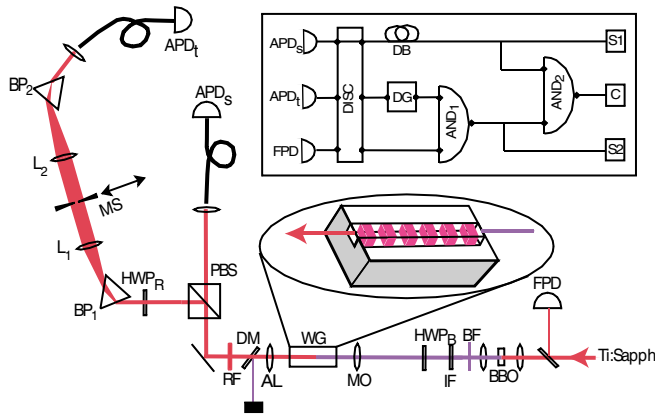


FIG. 1 (color online). Experimental apparatus with photon-counting electronics, including time-gating setup, shown in inset. A KTP nonlinear waveguide is set up to produce orthogonally polarized photon pairs via type-II PDC. A polarization beam splitter spatially splits the photon-pair sample; one spatial mode (trigger) is spectrally filtered and subjected to postdetection time gating while the signal mode is directly detected. FPD, fast photodiode; BBO, 2 mm  $\beta$ -barium-borate doubling crystal; BF, BG-39 Schott colored filter; IF, narrow-band pass filter; HWP<sub>B</sub>, half-wave plate set to flip polarization; MO, 10 $\times$  microscope objective; WG, 12 mm long KTiOPO<sub>4</sub> waveguide with 8.7  $\mu$ m period; AS, AR-coated  $f = 8$  mm aspheric lens; DM, blue-reflecting, red-transmitting dichroic mirror; RF, AR-coated RG-665 Schott colored filter; HWP<sub>R</sub>, AR-coated half-wave plate; PBS, polarizing beam splitter; BP<sub>1</sub> and BP<sub>2</sub>, Brewster-angle SF-10 prism; L<sub>1</sub> and L<sub>2</sub>,  $f = 10$  cm AR-coated lens; MS, translatable slit; APD<sub>t</sub>, trigger fiber-coupled avalanche photodiode (APD) from Perkin-Elmer; APD<sub>s</sub>, signal APD; INV, pulse inverter; DISC, pulse discriminator; DB, electronic variable delay line; DG, electronic delay generator (Stanford research DG-535); AND<sub>1</sub> and AND<sub>2</sub>, NIM AND gates; S<sub>1</sub>, S<sub>2</sub>, C, pulse counters.

focused using a 10 $\times$  microscope objective into the input face of a 12 mm long  $z$ -cut KTP waveguide formed by ion exchange (with 8.7  $\mu$ m grating period). The waveguide output is collimated and the remaining ultraviolet is filtered out from the PDC signal. The photon pairs are subsequently split by a polarizing beam splitter and the horizontally polarized signal mode is coupled by a multimode fiber to a commercial silicon-based avalanche photodiode (APD). The trigger channel (vertical polarization) is subjected to a low-loss prism spectrometer comprised of two SF-10 Brewster-angle prisms and two  $f = 10$  cm lenses; a motorized slit of adjustable width is placed at the Fourier plane whose position is computer controlled. The resulting trigger mode is similarly launched into a fiber-coupled APD. The slit position is calibrated by transmitting a titanium sapphire laser beam through the prism set up into a spectrometer, using a linear extrapolation for wavelengths outside the laser bandwidth. To implement time gating, a small percentage of the laser power is directed to a fast photodiode (1 ns rise time). The diode signal is amplified and discriminated, producing a train of pulses which is delayed (with an electronic delay generator) and combined at an AND gate with the discriminated trigger output, while a second AND gate compares the time-gated and nongated signals. All discriminators produce 3 ns NIM pulses and the minimum overlap at the AND gates to generate a coincidence pulse is 1 ns.

Waveguided PDC leads to several key advantages over PDC in bulk crystals because of accurate control of the spatial modes. Among these are increased source brightness and conditional preparation efficiencies limited only by detector losses. Despite the fact that in KTP the  $d_{24}$  element is considerably smaller in magnitude than those elements yielding type-I PDC ( $d_{33}$  and  $d_{31}$ ), it is possible to obtain a remarkably high production rate of type-II PDC photon pairs since the modes are confined within the cross section of the waveguide throughout the entire length of the structure. In our experiment one of the polarizations is regarded as a trigger, while we attempt to collect all photons in the orthogonal polarization (signal). In the limit of unit detector quantum efficiency together with vanishing optical losses and perfectly suppressed background, a trigger detection heralds the presence of a single photon in the signal arm. Such conditional detection is characterized by an efficiency given by the ratio of coincidence (trigger and signal) to single (trigger) detection rates. The source brightness, given by the coincidence rate per unit pump power, is an additional important measure of source performance, specifically in the context of concatenating multiple waveguides for quantum-optical networking.

We encountered two important sources of background photons produced by our waveguide. If not suppressed, such uncorrelated photons are a serious limitation to the conditional detection efficiency. First, the QPM grating needed for type-II PDC (with 8–10  $\mu$ m period) also

supports type-I PDC, resulting from the  $\chi^{(2)}$  elements  $d_{33}$  and  $d_{31}$ , producing same-polarization pairs which do not contribute to coincidence events and thus reduce the conditional detection efficiency. Fortunately, the various phase matched processes in the waveguide are spectrally distinct; indeed, we verified that a bandpass filter in the path of the ultraviolet pump can suppress type-I interactions. Second, the waveguide produces uncorrelated fluorescence photons, with an intensity comparable to that of PDC. The observed fluorescence is related to gray tracking in KTP due to color-center formation [18] and has been observed in PDC from bulk periodically poled material [19]. While in a waveguide a substantial fraction of the fluorescence is emitted into the supported modes, we found that the fluorescence and PDC signals exhibit certain features that can be exploited to differentiate between them. Our measurement showed that the fluorescence spectrum is considerably wider than that of PDC (130 nm vs 50 nm  $1/e$  full width). By filtering out frequencies at which PDC is not present, fluorescence is suppressed without appreciably reducing the PDC photon flux. Moreover, while PDC events occur within the femtosecond pump pulse window, fluorescence is emitted over much longer time scales. Therefore, gating in time with respect to the pump pulse train leads to further fluorescence suppression.

An experimental run consists of the recording of single and coincidence detection rates as a function of the slit position. A slit width of 40  $\mu\text{m}$  (giving a spectral resolution of 2 nm) maximizes the count rates at the maximum conditional preparation efficiency. Data were taken with and without time gating, as shown in Fig. 2(a). The maximum coincidence to singles ratio (i.e., the conditional detection efficiency) increases from 20.4% to 51.5% upon activation of time gating. The latter value represents the measured overall photon detection efficiency, including the effects of a nonunit quantum efficiency, imperfect optical transmission, and remaining uncorrelated photons due to fluorescence. If the heralded single photons are prepared for a subsequent experiment, rather than detected directly, the preparation efficiency need not include the signal detection loss, which together with imperfect fiber coupling is the highest source of loss (detector specifications indicate 60% quantum efficiency at 800 nm and measured fiber coupling efficiencies were  $>90\%$ ). For a quantum efficiency of 60%, a 51.5% conditional detection efficiency corresponds to a preparation efficiency of single photons close to 85%. The latter means that we can ascertain the presence of a single photon in a well-defined spatial mode with an 85% fidelity. Furthermore, annealing the color centers, e.g., by heating the waveguide [18], may suppress the remaining fluorescence and lead to nearly ideal single-photon preparation.

In a second experiment, we optimized the source brightness in order to maximize optical throughput while

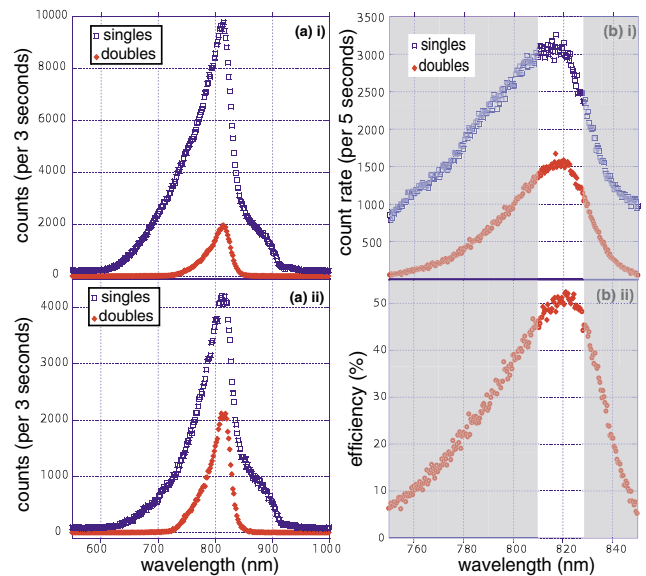


FIG. 2 (color online). (a) Spectrally resolved PDC. (i) Frequency-resolved single (trigger) and coincidence counts without time gating. Spectral filtering results in an increased maximum efficiency from  $\sim 11\%$  to  $\sim 20\%$ . (ii) Frequency-resolved single (trigger) and coincidence counts with time gating. Note that the maximum conditional detection efficiency increases from  $\sim 20\%$  to  $\sim 51\%$  upon activation of time gating. (b) Conditional detection efficiency for optimized source brightness. This figure shows spectrally resolved coincidences and single counts in the region of the coincidences peak. The unshaded band indicates the location and width (corresponding to a 17 nm spectral window) of the pump spectrometer slit yielding the highest brightness ( $8.5 \times 10^5$  coincidences/[s mW]) at the maximum conditional detection efficiency ( $\sim 51\%$ ). (i) depicts the frequency-resolved coincidence and single (trigger) detection rates. (ii) depicts the conditional detection efficiency (given by the ratio of coincidence to single counts).

retaining a high efficiency by adjusting the slit position and width, resulting in a 17 nm transmission window. For a 300 s integration time, we observed  $7.46 \times 10^5$  trigger,  $1.15 \times 10^7$  signal, and  $3.81 \times 10^5$  coincidence counts (the calculated accidental coincidence rate is  $<330$  counts) corresponding to a brightness of  $8.5 \times 10^5$  coincidences/(s mW). For comparison with our spectrally resolved measurements, Fig. 2(b) shows experimental data close to the coincidence peak; the unshaded band indicates the slit position and width corresponding to simultaneous brightness and efficiency maximization. We have thus shown the experimental realization of high-fidelity conditional preparation of fiber-coupled single photons generated by a femtosecond-pulse pumped KTP nonlinear waveguide [20] (in a microstructured optical array) based on orthogonally polarized PDC. Waveguiding leads to a high probability of photon-pair generation which translates into an extraordinarily high detection rate and a remarkable conditional efficiency. Although the produced single photons are characterized

by a broad spectral bandwidth, the temporal duration calculated to be  $\sim 20$  ps makes such photons far from Fourier-transform limited (such a temporal duration together with the spectral width given by the spectrometer slit corresponds to a time-bandwidth product of  $\sim 1000$ ). Fourier-transform behavior could be obtained in our setup by restricting further the trigger photon spectral width by adjusting the prism spectrometer slit. Given our high source brightness, the reduction of the available photon sample that would thus result could be compensated by an increased pump power. Additionally, an ultrashort pump enables synchronized emission from multiple sources to an accuracy of a few femtoseconds.

To our knowledge, the best previously reported ratio was obtained for polarization entangled pairs with cw-pumped PDC from a  $\beta$ -barium-borate crystal and collected with single-mode fibers (a very different configuration from ours) was 28.6% at a brightness of 775 counts/(s mW) [21]. The lack of a classical timing signal for this source makes multiple source synchronization difficult. Experiments aimed at determining the quantum efficiency of single-photon detectors have reported high coincidence to singles ratios [22] when corrected for optical losses; however, photons in the signal arm were not in a single spatial mode, limiting the potential for usable conditionally prepared single photons. We believe that our higher brightness arises from accurate modal definition at the source, leading to efficient fiber coupling of the whole photon sample. In contrast, for bulk crystal PDC, mode definition is possible only *a posteriori* (e.g., with irises or fibers).

Further development of our source could include modal engineering of the conditionally prepared photons to yield well-defined pure photon-number states (i.e., Fock states) and arbitrary superposition wave packets [23,24]. Mode matching into single-mode fibers should be straightforward given that the waveguide exhibits accurate spatial mode control. The high degree of correlations of the generated photon pairs should enable improved experiments designed for tests of local realism. Precise timing together with high brightness paves the road towards concatenation of multiple waveguides in integrated quantum-optical networks. Our observed high brightness together with the use of an ultrashort pump could lead to source scalability by utilizing multiwaveguide arrays. In addition, such high brightness permits the generation of higher-occupancy Fock states at experimentally usable production rates. In conclusion, our source is an ideal building block for quantum information applications offering compatibility with all-fiber systems, while room-temperature operation makes it a convenient alternative to solid-state sources.

This work was supported by ARDA under Grant No. P-43513-PH-QCO-02107-1. A. U. acknowledges support from the Center for Quantum Information, which is funded by ARO administered MURI Grant No. DAAG-19-99-1-0125. We acknowledge useful discussions with

C. Radzewicz.

- 
- [1] I. Bialynicki-Birula, in *Progress in Optics XXXVI*, edited by E. Wolf (Elsevier, Amsterdam, 1996).
  - [2] A. I. Lvovsky *et al.*, Phys. Rev. Lett. **87**, 050402 (2001).
  - [3] E. Knill, R. LaFlamme, and G. J. Milburn, Nature (London) **409**, 46 (2001); T. C. Ralph, A. G. White, W. J. Munro, and G. J. Milburn, Phys. Rev. A **65**, 012314 (2001); T. B. Pittman, M. J. Fitch, B. C. Jacobs, and J. D. Franson, quant-ph/0303095.
  - [4] P. G. Kwiat *et al.*, Phys. Rev. Lett. **75**, 4337 (1995); G. Weihs, T. Jennewein, C. Simon, H. Weinfurter, and A. Zeilinger, Phys. Rev. Lett. **81**, 5039 (1998).
  - [5] J. L. O'Brien, G. J. Pryde, A. G. White, T. C. Ralph, and D. Branning, Nature (London) **426**, 264 (2003).
  - [6] A. B. U'Ren, K. Banaszek, and I. A. Walmsley, Quantum Inf. Comput. **3**, 480 (2003).
  - [7] D. Bouwmeester *et al.*, Nature (London) **390**, 575 (1997); D. Boschi *et al.*, Phys. Rev. Lett. **80**, 1121 (1998).
  - [8] J. W. Pan, D. Bouwmeester, H. Weinfurter, and A. Zeilinger, Phys. Rev. Lett. **80**, 3891 (1998).
  - [9] H. J. Briegel, W. Dür, J. I. Cirac, and P. Zoller, Phys. Rev. Lett. **81**, 5932 (1998).
  - [10] See, for example, a review: N. Gisin, G. G. Ribordy, W. Tittel, and H. Zbinden, Rev. Mod. Phys. **74**, 145 (2002).
  - [11] C. Kurtsiefer, S. Mayer, P. Zarda, and H. Weinfurter, Phys. Rev. Lett. **85**, 290 (2000).
  - [12] P. Michler *et al.*, Science **290**, 2282 (2000); Z. Yuan *et al.*, Science **295**, 102 (2002); C. Santori, D. Fattal, J. Vuckovic, and Y. Yamamoto, Nature (London) **419**, 594 (2002).
  - [13] A. Kuhn, M. Hennrich, and G. Rempe, Phys. Rev. Lett. **89**, 067901 (2002).
  - [14] B. Lounis and W. E. Moerner, Nature (London) **407**, 491 (2000).
  - [15] M. Barberi, F. De Martini, G. Di Nepi, and P. Mataloni, Phys. Rev. Lett. **92**, 177901 (2004).
  - [16] K. Banaszek, A. B. U'Ren, and I. A. Walmsley, Opt. Lett. **26**, 1367 (2001); S. Tanzilli *et al.*, Electron. Lett. **37**, 26 (2001); K. Sanaka, K. Kawahara, and T. Kuga, Phys. Rev. Lett. **86**, 5620 (2001); M. C. Booth *et al.*, Phys. Rev. A **66**, 023815 (2002).
  - [17] M. E. Anderson, M. Beck, M. G. Raymer, and J. D. Bierlein, Opt. Lett. **20**, 620 (1995).
  - [18] B. Boulanger *et al.*, IEEE J. Quantum Electron. **35**, 281 (1999).
  - [19] C. E. Kuklewicz, M. Fiorentino, G. Messin, F. N. C. Wong, and J. H. Shapiro, Phys. Rev. A **69**, 013807 (2004).
  - [20] M. G. Roelofs, A. Suna, W. Bindloss, and J. D. Bierlein, J. Appl. Phys. **76**, 4999 (1994).
  - [21] C. Kurtsiefer, M. Oberparleiter, and H. Weinfurter, Phys. Rev. A **64**, 023802 (2001).
  - [22] P. G. Kwiat *et al.*, Phys. Rev. A **48**, R867 (1993).
  - [23] W. P. Grice, A. B. U'Ren, and I. A. Walmsley, Phys. Rev. A **64**, 063815 (2001).
  - [24] M. Dakna, J. Clausen, L. Knöll, and D. G. Welsch, Phys. Rev. A **59**, 1658 (1999); D. T. Pegg, L. S. Phillips, and S. M. Barnett, Phys. Rev. Lett. **81**, 1604 (1998).